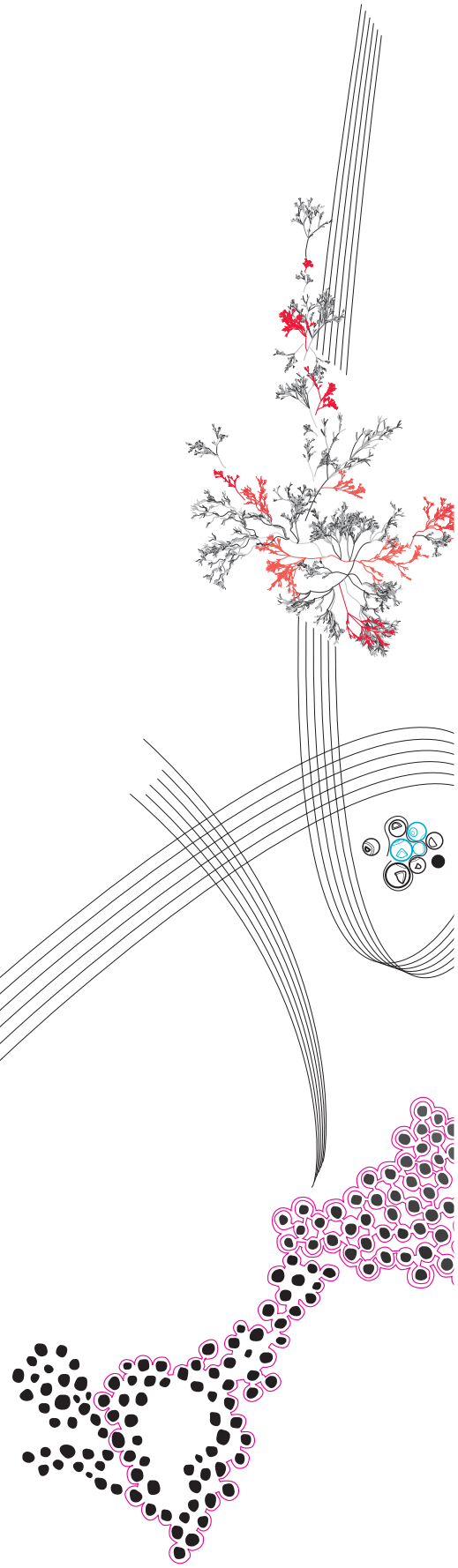

BSc Thesis Applied Mathematics

Approximating Integrals within General 2D Curved Domain

Jelle Boon

Supervisor: Carlos Pérez Arancibia

August, 2023

Department of Applied Mathematics
Faculty of Electrical Engineering,
Mathematics and Computer Science

UNIVERSITY OF TWENTE.

Preface

This paper was written as Bachelor's Assignment. I want to thank Carlos Pérez Arancibia for supervising and guiding me throughout this period. I also really enjoyed looking further into interpolatory quadrature, as this has not been discussed in my Bachelor's programme. Enjoy!

Approximating Integrals within General 2D Curved Domain

Jelle Boon

August, 2023

Abstract

This thesis presents an argument for super-algebraic convergence of two numerical quadrature rules that estimate double integrals of analytic functions with a complex domain. The approach is based on the 1D quadrature rules (Fejér's first and Clenshaw-Curtis). Finally, it will show that the numerical results converge super-algebraically.

Keywords: Transfinite Interpolation, Chebyshev Polynomials, numerical quadrature, Fejér first rule, Clenshaw-Curtis Quadrature, Convergence rate

1 Introduction

Many problems in physics and engineering rely on partial differential equations. These problems can often be addressed by reformulating the original problem as integro-differential equations [6]. To solve these, an appropriate discretisation of the domain is needed to apply high-order quadrature rules and numerical differentiation. In this thesis, we make use of Chebyshev grids which allow spectrally accurate differentiation and integration of sufficiently smooth functions. Here we focus on the integration part: How to best approximate integrals within a general 2D Curved Domain?

In the field of numerical mathematics, Chebyshev grids have been around for a while. Fejér proposed his first and second quadrature rules in 1933 [2] and Clenshaw and Curtis proposed their rule in 1960 [12]. Furthermore, S. Xiang and L. Trefethen have done extensive research into the error bounds of these quadrature rules [11] [16] [15]. There are multiple ways to derive appropriate discretisations of general 2D domains: Conformal maps [10], finite element method and transfinite element method [7] for example. For the transfinite element method, one needs to make domain decompositions. HOHQ-mesh software has been developed [8] to do this generally. However, this is beyond this thesis. Therefore, we construct the decomposition ourselves.

In this thesis, we will numerically approximate an integral within a complex domain by combining the ideas proposed above. We will first make a patch decomposition of our domain, for which we will make mappings to a suitable domain for high-order spectral methods. Over these domains, we will apply the quadrature rules.

In section 2 we will discuss the transfinite interpolation and its exact mapping formula. Furthermore, we will introduce the domains that we will discuss in this thesis. In section 3, the Chebyshev series and its convergence will be discussed. These results are needed for the convergence of the quadrature rules. Section 4 will discuss the two applied quadrature rules, their weight derivations and their convergence. The last part of section 4 argues why we can apply the 1-dimensional quadrature rules twice over our patches. Section 5 goes into the numerical results. The approximations will be tested using Green's theorem, where the contour integral of our domain will be calculated exactly and our approximation integrates a function which takes the value of 1 for all inputs.

2 Transfinite Interpolation

We will construct a patch representation of simply connected domains $\Omega \subset \mathbb{R}^2$, with a given parameterised curve as boundary ($\Gamma = \partial\Omega$). The boundary Γ is assumed to be parameterized by the smooth 2π-periodic function $\gamma : [0, 2\pi] \mapsto \Gamma$. Let us denote the patches as $\{\Omega_1, \Omega_2, \dots\}, \Omega_i \subset \Omega$. Here $\Omega = \bigcup_i \Omega_i$ and $\emptyset = \bigcap_i \Omega_i$. There will be a mapping (Ψ_i) associated with each of these patches: $\Psi_i : [-1, 1]^2 \mapsto \Omega_i$. This mapping will be constructed using transfinite interpolation, which makes sure that the mapping is bijective and continuous. In this thesis we will consider five specific curves:

$$x_C(t) = \cos t, \qquad y_C(t) = \sin t \tag{1}$$

$$x_E(t) = 2\cos t, \qquad y_E(t) = \sin t \tag{2}$$

$$x_K(t) = \cos(t) + 0.65\cos(2 * t) - 0.65, \qquad y_K(t) = 1.5\sin t \tag{3}$$

$$x_S(t) = \cos(t)r(t), \qquad y_S(t) = \sin(t)r(t) \tag{4}$$

$$\textit{where, } r(t) = 0.3\cos(5t - \pi/2)$$

$$x_J(t) = \cos(t)s(t), \qquad y_J(t) = \sin(t)s(t) \tag{5}$$

$$\textit{where, } s(t) = 1 + 0.3\cos\left(4[t + 0.5\sin(t)]\right)$$

where C, E, K, S and J stand for circle, ellipse, kite, star and jellyfish respectively.

2.1 Construction of patches

For the sake of simplicity, we will construct the patches by hand in this thesis. We want to construct patches, where the boundary consists of four curves that can be parameterized. The easiest way to do this is to construct a square in the middle of our domain and connect its corners to points on the boundary. This results in five patches that suit our preferences. The resulting patches generated for a circle and star-shaped domains are sown in Figure 1, where each patch is coloured differently. Here the corners of the square have been connected with the points on the circle nearest to them, i.e., the corresponding points on the circle correspond to the orthogonal projection of the corners onto the domains' boundary.

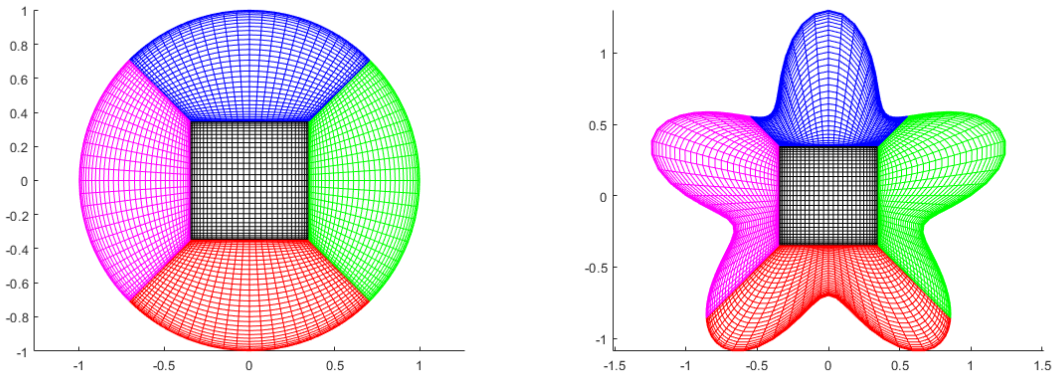

(A) Circle (B) Star

FIGURE 1: Patch Decomposition

2.2 Transfinite Interpolation Function

Having constructed our patches, let us at a specific patch Ω_i. Let $(\partial\Omega_i)_j,\ j \in \{t, b, l, r\}$ denote the four pieces of the boundary, where j denotes the *bottom, top, left* and *right* of the patch respectively. *The specific choice of orientation does not matter, as long as the top and bottom are opposite to each other.* These boundaries are then either part of the boundary or straight lines. In both cases they are parametrizable.

Let $\psi_i^j : [-1, 1] \mapsto (\partial\Omega_i)_j,\ j \in \{t, b, l, r\}$

$$\psi_i^b(u),\ \psi_i^t(u), \quad -1 \le u \le 1, \qquad \psi_i^l(v),\ \psi_i^r(v), \quad -1 \le v \le 1, \tag{6}$$

where their corners are connected, such that their parametrizations run in the same direction, i.e.

$$\begin{aligned} \psi_i^b(-1) &= \psi_i^l(-1), & \psi_i^b(1) &= \psi_i^r(-1), \\ \psi_i^t(1) &= \psi_i^r(1), & \psi_i^t(-1) &= \psi_i^l(1). \end{aligned} \tag{7}$$

Now that we have parameterized the boundaries of the patches, we can construct mappings for our patches. Here, we do so by applying transfinite interpolation [7]. Originally a domain of $[0, 1]$ is used. Meaning that we had to adapt the function for our $[-1, 1]$ domain. This results in the following formula:

$$\begin{aligned} \Psi_i(u, v) = \frac{1}{2}\big[\ &(1 - v)\psi_b(u) + (1 + v)\psi_t(u) + (1 - u)\psi_l(v) + (1 + u)\psi_r(v)\ \big] \\ &- \frac{1}{4}\big[\ (1 + u)(1 + v)\psi_t(1) + (1 + u)(1 - v)\psi_b(1) \\ &\quad + (1 + v)(1 - u)\psi_t(0) + (1 - u)(1 - v)\psi_b(0)\ \big] \end{aligned} \tag{8}$$

2.3 Smooth Mapping

Now let $f[X]$ denote the image under f of X, i.e. $f[X] := \{f(x),\ x \in X\}$. If we now look at our boundary curves as maps, i.e. $\psi_i^j : [-1, 1] \mapsto \psi_i^j[-1, 1],\ j = t,\ b,\ l,\ r$. These curves can either be straight lines or are a part of the boundary curve of our domain. We can easily see that if $\psi_i^j[-1, 1]$ is a straight line, ψ_i^j is a bijective continuous map. Since we assume that our domain is simply connected, the border $(d\Omega)$ can be seen as a Jordan curve. This curve can also be seen as the image of a continuous injective map $d\Omega : [0, 1] \to \mathbb{R}^2$, since it is a homeomorphism of the unit-circle [5]. If ψ_i^j is part of the border, we, therefore, know it is continuous. Furthermore, since we said that $\psi_i^j : [-1, 1] \mapsto \psi_i^j[-1, 1]$ and $d\Omega : [0, 1]$ is injective, we can conclude that ψ_i^j also is a continuous bijective map.

Finally, since $\Psi_i : [-1, 1] \mapsto \Omega_i$ is a combination of continuous bijective maps, we can also conclude that it also is (Theorem 3.22 [13]). This result is used to justify the calculation of the Jacobian and the use of Ψ_i^{-1}.

2.4 Domain Decomposition

Given domain $\Omega \subset \mathbb{R}^2$ with patches $\{\Omega_1, \ldots, \Omega_n\}$ and analytic function $F(x, y),\ (x, y) \in \Omega$. We take our mappings $\Psi_i : [-1, 1]^2 \mapsto \Omega_i$ from (8). Since our mappings are invertible and bijective, we can make calculate the Jacobian. Using that and the additivity of domains [1], we have:

$$\iint_\Omega F(x, y)dxdy = \sum_{i=1}^{n} \iint_{\Omega_i} F(x, y)dxdy = \sum_{i=1}^{n} \iint_{[-1,1]^2} F(\Psi_i(u, v)) \left|\frac{\partial(x, y)}{\partial(u, v)}\right| dudv. \tag{9}$$

The implementation of the Jacobian in our quadrature rule means that we also need to accurately. If it is not too difficult, one could calculate the Jacobian analytically for each patch. Otherwise, one could calculate the Jacobian numerically up to a certain accuracy, which will limit the accuracy of the quadrature rule. In this thesis the choice has been made to do this numerically, meaning that our error will be bounded.

We have also decided to construct the patches ourselves. While this approach is general, we do it by hand. There is HOHQMesh-software which can do this for you, however, that was out of the scope of this thesis [8]. An example of such a domain decomposition is in Figure 2.

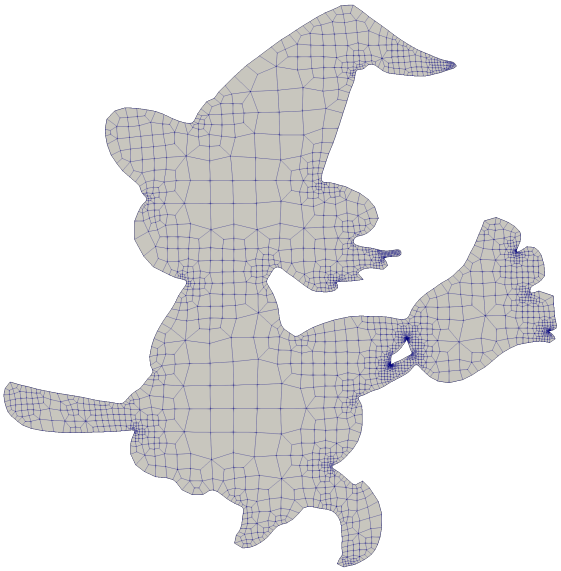

FIGURE 2: Patch Decomposition Witch [8]

3 Chebyshev Series

3.1 Chebyshev Polynomials

A Chebyshev polynomial can be defined as the real part of the function z^k on the unit circle. Below is the equation for the k^{th} Chebyshev polynomial.

$$T_k(x) = \frac{1}{2}(z^k + z^{-k}) = \cos(k\theta)$$

Since $T_0(x), T_1(x), \ldots$ for a basis for $\mathcal{P}_n$, any polynomial p can be written uniquely as a finite Chebyshev series [12].

$$f(x) = \sum_{k=0}^{\infty} a_k T_k(x), \text{ with } a_k = \frac{2}{\pi}\int_{-1}^{1} \frac{f(x)T_k(x)}{\sqrt{1-x^2}}dx \text{ for } k > 0, \tag{10}$$

and for $k = 0$ by by the same formula with the factor $2/\pi$ changed to $1/\pi$.

3.1.1 Convergence of Chebyshev Series

It turns out that a Chebyshev series always converges geometrically if all its derivatives are bounded on the interval $x \in [-1, 1]$.

We can show that by the following argument (from [11]), where we first substitute $x = \cos\theta$ as follows and start with the assumption that the first (j)-derivatives are absolutely continuous, and the $(j+1)^{\text{th}}$ is bounded by some $V < \infty$.

$$a_k = \frac{2}{\pi}\int_{-1}^{1} \frac{f(x)T_k(x)}{\sqrt{1-x^2}}dx \tag{11}$$

$$= -\frac{2}{\pi}\int_{\pi}^{0} \frac{f(\cos\theta)\cos(k\theta)}{\sqrt{1-\cos(\theta)^2}}\sin\theta d\theta$$

$$= \frac{2}{\pi}\int_{0}^{\pi} f(\cos\theta)\cos(k\theta)d\theta \tag{12}$$

When integrating Equation 12 by parts, we get:

$$a_k = \frac{2}{k\pi}\left[f(\cos\theta)\sin(k\theta)\right]_0^\pi + \frac{2}{k\pi}\int_0^\pi f'(\cos\theta)\sin\theta\sin(k\theta)d\theta \tag{13}$$

$$= \frac{2}{k\pi}\int_0^\pi f'(\cos\theta)\sin\theta\sin(k\theta)d\theta \tag{14}$$

Here the first term vanishes, since $\sin(k\pi) = 0,\ \forall k \in \mathbb{Z}$. Note that this is exact when using integration-by-parts is justified. Since $f(x)$ must be smooth enough for its first derivative to be integrable.

Furthermore, we can notice that $2\sin\theta\sin(k\theta) = \cos(k\theta - \theta) + \cos(k\theta + \theta)$ [1]. If we insert this into Equation 14, we get:

$$a_k = \frac{2}{k\pi}\int_0^\pi f'(\cos\theta)\left[\frac{\cos(k\theta-\theta)}{2} + \frac{\cos(k\theta+\theta))}{2}\right]d\theta \tag{15}$$

Take note that the term on the right will never exceed 1. Therefore its L^∞ norm is bounded by 1. Meaning that we can rewrite this into

$$|a_k| \leq \frac{2}{n\pi}\|f'(\cos\theta)\|_1 \left\|\frac{\cos(k\theta-\theta)}{2} + \frac{\cos(k\theta+\theta))}{2}\right\|_\infty \leq \frac{2}{n\pi}\|f'(\cos\theta)\|_1 \tag{16}$$

Now we can say that $|a_k| \leq 2V_1/k\pi$, where $V_1 = \|f^{(1)}(\cos\theta)\|_1$. Where we use a (1) to denote the first derivative. If then we can take further steps with our integration by parts, we would introduce higher and higher derivatives of f up till $j+1$. Where $V_{j+1} = \|f^{(j+1)}(\cos\theta)\|_1$. Furthermore, we would introduce more and more cosines. However, in the same way, their L^∞ norm would be upper bounded by 1. Lastly, we introduced a k term in the first integration by parts. For the next one, we can see from Equation 15, we would introduce $k+1$ and $k-1$. The third factor will be $k-2, k$ and $k+2$, on and on and on. To make the formula easier, we weaken it slightly by only including the negative decreasing factors: $k, k-1, k-2, \ldots, k-j$. This leaves us with the formula

$$|a_k| \leq \frac{2V}{\pi k(k-1)\cdots(k-j)}, \tag{17}$$

where $f, f', \ldots f^{(k)}$ are absolutely differentiable on $[-1,1]$ and $f^{(k+1)} = V < \infty$ for $n-1 \geq k \geq 0$. Here $|a_k|$ are thus of order $O(Vk^{-j-1})$. This is needed later in section 4.2.

If we now change our assumption to f is analytic, and this is absolutely continuous and bounded for all its derivatives, then our derivation implies that for large k the coefficients are decreasing faster than any finite power of k. This is the property of exponential or geometric convergence. Therefore a Chebyshev series converges super-algebraic for analytic functions. This last argument is borrowed from [2], where it is used to argue that Fourier series converge super-algebraic in the same way.

Finally, it can be shown that for analytic functions, it is actually geometric convergence [12]. However, this proof is beyond the scope of this thesis.

4 Interpolatory Quadrature Rules

In a standard quadrature problem, we start with a function $f \in C[-1,1]$ which we want to integrate over the interval $[-1,1]$. We start with a given $n \geq 0$. Then we pick $n+1$ *nodes* at which we sample f. Then we approximate I by integrating the polynomial p_n of degree n which interpolates these nodes. This integral is denoted as I_n. Instead of constructing and integrating p_n, we calculate it using the formula below. The numbers $w_0, \ldots, w_n$ are weights that are determined, based on our chosen nodes, such that I_n will be correctly calculated and x_k are our chosen nodes [12].

$$I[f] = \int_{-1}^{1} f(x)dx \qquad I_n[f] = \int_{-1}^{1} p_n(x)dx = \sum_{k=0}^{n} w_k f(x_k) \tag{18}$$

When using Chebyshev polynomials, there are two logical options for nodes: their zeros and their extremes. These are our choice of nodes for Fejér's first and Clenshaw-Curtis quadrature rules [3].

$$x_k^F = \cos\theta_k, \qquad \theta_k^F = \frac{2k-1}{2n}\pi, \qquad k = 1, 2, \ldots, n \tag{19}$$

$$x_k^{CC} = \cos\theta_k, \qquad \theta_k^{CC} = \frac{k}{n}\pi, \qquad k = 0, 1, \ldots, n \tag{20}$$

These weights can be calculated using classical methods. However, Waldvogel showed that these weights can also be calculated using the inverse discrete Fourier transform. This reduces our order of operations from $O(n^2)$ to $O(n \log n)$ [14].

4.1 Fejér Weight Derivations

Since these are interpolatory rules, it can be shown that w_k^F can be calculated by the equation below [3].

$$w_k^F = \frac{1}{T_n'(x_k^F)} \int_{-1}^{1} \frac{T_n(x)}{x - x_k^F} dx \tag{21}$$

Furthermore, we can rewrite T_n using the Christoffel-Darboux formula [4], with $y = x_k^F$.

$$1 + 2\sum_{j=1}^{n-1} T_j(x)T_j(x_k^F) = -\frac{T_n(x)T_{n+1}(x_k^F)}{x - x_k^F}$$

Which allows us to conclude from (21) that,

$$w_k^F = \frac{2}{T_n'(x_k^F)T_{n+1}(x_k^F)} \left[1 + \sum_{j=1}^{n-1} T_j(x_k^F) \int_{-1}^{1} T_j(x)dx \right] \tag{22}$$

Now using $T_n'(\cos\theta = n(\sin n\theta)/\sin\theta$, we get

$$T_n'(x_k^F) = T_n'(\cos\theta_k^F) = (-1)^{k-1} n/\sin\theta_k^F,$$
$$T_{n+1}(x_k) = \cos(n+1)\theta_k^F = (-1)^k \sin\theta_k^F.$$

The integral can also be calculated algebraically,

$$\int_{-1}^{1} T_j(x)dx = \int_0^{\pi} \cos j\theta \sin\theta d\theta = \begin{cases} 2/(1-j^2), & \textit{if } j \textit{ is even,} \\ 0, & \textit{if } j \textit{ is odd.} \end{cases}$$

Combining these equations with what we had in (22), we conclude that

$$w_k^F = \frac{2}{n}\left[1 - 2\sum_{j=1}^{[n/2]} \frac{\cos\left(2j\theta_k^F\right)}{4j^2-1}\right], \qquad k = 1, 2, \ldots, n \tag{23}$$

4.1.1 Clenshaw-Curtis Weights

A similar derivation can be done for w_k^{CC}. For a full derivation, see [9]. Here, we will use the notation that is also given in [14], to remain constant with our terminology.

$$w_k^{CC} = \frac{c_k}{n}\left(1 - \sum_{j=1}^{[n/2]} \frac{b_j}{4j^2-1}\cos(2j\theta_k^{CC})\right), \qquad k = 0, 1, \ldots, n \tag{24}$$

$$\text{with } b_j = \begin{cases} 1, & j = n/2, \\ 2, & j < n/2, \end{cases} \text{ and } c_k = \begin{cases} 1, & k = 0 \mod n, \\ 2, & \text{otherwise} \end{cases} \tag{25}$$

4.2 Convergence of Quadrature

First, we are going to show the super-algebraic convergence of the Clenshaw-Curtis quadrature, after which we argue for the same rate of convergence for Fejer. For this, we do the same as in section 3.1.1. We start with the assumptions that the first (k)-derivatives are absolutely continuous and the $(j+1)^{\text{th}}$ is bounded by some $V < \infty$, which we will later change into f is analytic. In this instance the argument is derived in [11].

We start with the fact that the quadrature error can be written as [11],

$$I(f) - I_n(f) = \sum_{k=0}^{\infty} a_k(I[T_k] - I_n[T_k]) \tag{26}$$

Thus, the absolute value of the quadrature error can be upper bounded as follows

$$|I[f] - I_n[f]| \leq \left|\sum_{k=0}^{\infty} a_k(I[T_k] - I_n[T_k])\right| \tag{27}$$

$$= \sum_{k=0}^{n} |a_k||I[T_k] - I_n[T_k]| \tag{28}$$

$$+ \sum_{k=n+1}^{2n-\lfloor n^{1/3}\rfloor} |a_k||I[T_k] - I_n[T_k]| \tag{29}$$

$$+ \sum_{k=2n+1-\lfloor n^{1/3}\rfloor}^{2n+1} |a_k||I[T_k] - I_n[T_k]| \tag{30}$$

$$+ \sum_{k=2n+2}^{\infty} |a_k||I[T_k] - I_n[T_k]| \tag{31}$$

Now let us denote the sums in Equations 28 till 31 as S_1, S_2, S_3 and S_4 respectively. Also, note that S_1 is zero since our quadrature formulas are interpolatory. The reason for choosing these sums will be justified later.

Now we want to set upper bounds for $I(T_{n+p}) - I_n(T_{n+p})$, with $p \geq 0$. For that, we are going to look at some symmetry: When taking taking the points $\theta_i = \pi j/n,\ 0 \leq i \leq 2n-1$,

it can be shown that for any $p \in \mathbb{Z}$, $\cos([n+p]\pi\theta_i) = \cos([n-p]\pi\theta_i)$. This leads us, when using $x_i = \cos\theta_i$, to the result that

$$T_{n+p}(x_i) = T_{n-p}(x_i) \quad (0 \leq j \leq n) \tag{32}$$

Therefore, on a Chebyshev grid, this equality holds. This can then be estimated by first using that $\int_{-1}^{1} T_k(x)dx = 2/(1-k^2)$ (for even j), to arrive at

$$I_n(T_{n+p}) = I_n(T_{n-p}) = I(T_{n+p}) = \begin{cases} 0, & \text{if } n \pm p \text{ is odd,} \\ \frac{2}{1-(n-p)^2}, & \text{if } n \pm p \text{ is even.} \end{cases} \tag{33}$$

However, this is point-wise for x_i and not the whole interval. Therefore there will be some errors by integrating using T_{n-p}. Which can also be used to estimate the error that we made by doing that for both integrals,

$$I(T_{n+p}) - I_n(T_{n+p}) = \begin{cases} 0, & \text{if } n \pm p \text{ is odd,} \\ \frac{8pn}{n^4-2(p^2+1)n^2+(p^2-1)^2}, & \text{if } n \pm p \text{ is even.} \end{cases} \tag{34}$$

Going back to S_2, which consists of $O(n)$ terms. Also, we can use Equation 34 to see that $|I(T_k) - I_n(T_k)|$ these are in the worst case $O(n^{-2/3})$. In Section 3.1.1 we showed that a_k are $O(Vn^{-j-1})$. Concluding that S_2 has a total magnitude of $O(Vn^{-j-2/3})$. Similarly, we can construct a total magnitude for S_3. It has $O(n^{1/3})$ terms, sizes $O(Vn^{-j-1})$, which again results in total magnitude $O(Vn^{-j-2/3})$ Meaning that $S_2 + S_3$ also has magnitude $O(Vn^{-j-2/3})$

Then we have only S_4 left. It can be shown that $|I(T_k) - I_n(T_k)| \leq 32/15$ for $k \geq 4$, which is done in [12]. Now combining this with Equation 17, we get

$$|I[f] - I_n[f(u_i)]| = S_1 + S_2 + S_3 + S_4 \tag{35}$$

$$\leq 0 + O(Vn^{-k-2/3}) + \frac{32V/15}{\pi j(2n+1-j)^j} \tag{36}$$

Finally, we change our assumption to f is analytic, which similarly as in section 3.1.1 implies that our interpolatory quadrature converges super-algebraic to exact integral. It can also be shown that this convergence is geometric [12]. This is beyond this thesis.

Also, note that this derivation was only for the Clenshaw-Curtis quadrature. It can be shown that Fejér's first quadrature rule has the same order of convergence as Clenshaw-Curis [15]. Therefore, the quadrature error of Fejér will also decay at least super-algebraically.

4.3 2 Dimensions

Now that we have a way to super-algebraically estimate a 1D-integral, we have to look at a way to apply that to our Equation 9. We will solve our 2D-integral by first fixing one variable (u) and by defining a function $g(u)$ that is the integral over v.

$$\begin{aligned} \iint_A F(\xi)dA &= \iint_{[-1,1]^2} f(u,v)dudv, \text{ where } f(u,v) = F(X(\xi))J_X(\xi) \\ &= \int_{-1}^{1} g(u)du, \text{ with } g(u) = \int_{-1}^{1} f(u,v)dv \end{aligned} \tag{37}$$

We can now clearly see that our double integral has been split up into two separate integrals. This same separation can be applied to our interpolation. Since $f : [-1,1]^2 \to \mathbb{R}$ is a C^∞ function of both (u,v), we have that the function $f(u,\cdot) : [-1,1] \to \mathbb{R}$, is also a C^∞ function over v. Therefore, we can apply our quadrature rules to $f(u,\cdot)$, which will be denoted by $g_n(u)$. We will use w_j as a placeholder for w_j^F from (23) or w_j^{CC} from (24) and x_j for x_j^F from (19) or x_j^{CC} from (20), depending on the choice of quadrature.

$$g_n(u) = I_n[f(u,\cdot)] = \sum_{j=0}^{n} w_j f(u, x_j), \tag{38}$$

Similarly, since $f : [-1,1]^2 \to \mathbb{R}$ is a C^∞ function of both (u,v), we have that for all $j = 1, \ldots, n$, the function $f(\cdot, x_j) : [-1,1] \to \mathbb{R}$, is also a C^∞ of u. $g_n(u)$ can be seen as a weighted sum of C^∞ functions. Therefore, by Theorem 3.22 [13] we can say that $g_n(u)$ is also a C^∞ function.

$$I_n[f] = \sum_{i=0}^{n} w_i g_n(x_i), \text{ with } g_n(u) := I_n[f(u,\cdot)] = \sum_{j=0}^{n} w_j f(u, x_j), \tag{39}$$

$$I_n[f] = \sum_{i=0}^{n} w_i \sum_{j=0}^{n} w_j f(x_i, x_j), \text{ where } f(u,v) = F(X(\xi))J_X(\xi) \tag{40}$$

where w_j is a placeholder either w_j^F from (23) or w_j^{CC} from (24) and similarly x_j for either x_j^F from (19) or x_j^{CC} from (20), depending on the choice of quadrature rule.

4.3.1 Convergence of 2D Quadrature

When looking at (39), we know that $g_n(u)$ converges super-algebraically to $g(u)$ by section 4.2. Since we have already argued that we can also apply our quadrature to $g_n(u)$, we have a super-algebraic converging series of another super-algebraic series. Therefore, we state that our $I_n[f]$ therefore also converges super-algebraically.

$$I[f] = \iint_A F(z)dA = \sum_{i=1}^{5} \iint_{[-1,1]^2} f(u,v)dudv$$

$$I_n[f] = \sum_{k=0}^{n} w_k \sum_{j=0}^{n} w_j f(x_k, x_j), \text{ where } f(u,v) = F(\Psi_i(z))J_{\Psi_i}(z)$$

5 Numerical Results

Now that we have theoretically shown that it is possible to estimate analytic functions super-geometrically, we can also check this numerically. This will be done using Green's theorem, where we solve the contour integral exactly and the area integral numerically. Meaning that we can calculate the exact error the quadrature gives us.

5.1 Area Test

If $\mathcal{C}$ is a positively oriented, piece-wise smooth, simple closed curve bounding a region R in the plane, then, by Green's Theorem [1].

$$\oint_{\mathcal{C}} x dy = -\oint_{\mathcal{C}} y dx = \frac{1}{2}\oint_{\mathcal{C}} x dy - y dx = \iint_R 1 dA$$

Then we can algebraically determine the exact value of the area of R. Now the absolute difference between our estimation and our exact value is our absolute error.

$$E\big[I_n[f]\big] = \left| I_n[f] - \frac{1}{2}\oint_{\mathcal{C}} x dy - y dx \right| \tag{41}$$

5.2 Choice of Curves

In section 2, we have discussed the five different curves that we consider in this thesis. As a reminder, these are a circle, an ellipse, a kite, a star and a jellyfish. The parametrizations of the boundary curves are also given in that section, together with the domain decomposition of a circle and a star. These figures depict the patches using a Chebyshev grid of 32 points. Below are the domain decompositions of the ellipse, kite and jellyfish.

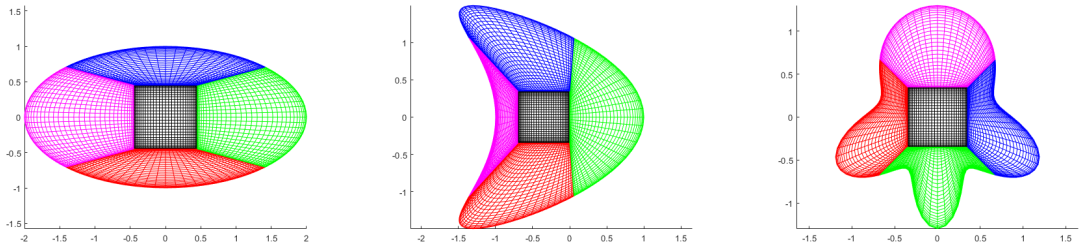

(A) Ellipse (B) Kite (C) Jellyfish

FIGURE 3: Patch Decomposition (2)

5.3 Results

The area integrals of these curves can be calculated algebraically. Below are the plots of the absolute error against $2 \leq n \leq 32$ with a given $h = 1e-5$ (the stepsize for our Jacobean) for each of the curves above. What we see here is that the error goes down super-algebraically up till a certain threshold, where it stabilises. This can be explained by the fact that the Jacobean is calculated with a finite difference step.

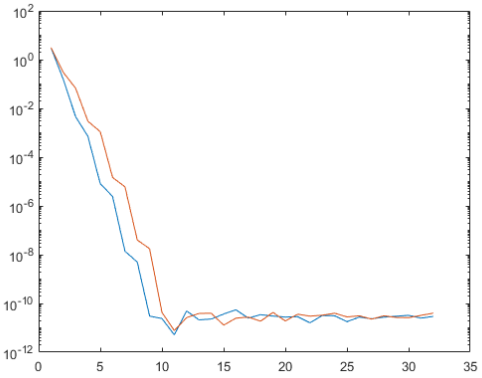

(A) Semilogplot

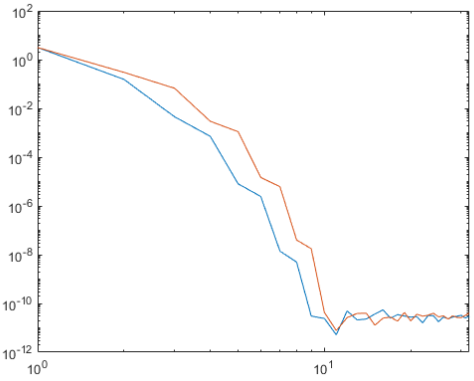

(B) Logplot

FIGURE 4: Area Tests Circle

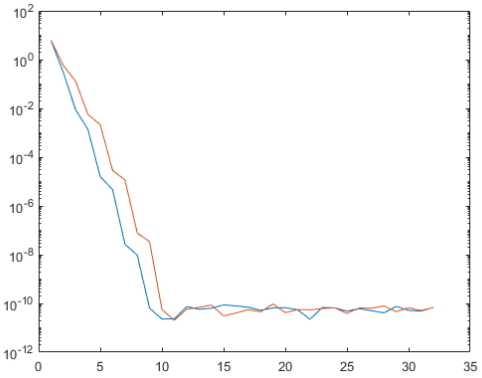

(A) Ellipse

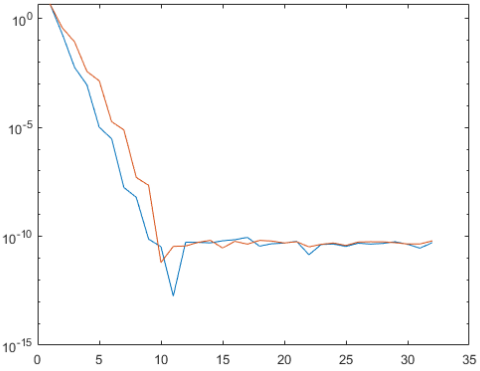

(B) Kite

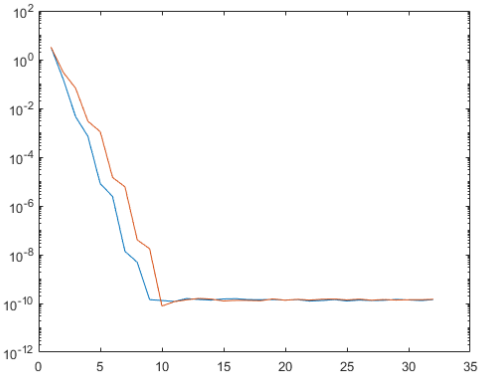

(C) Star

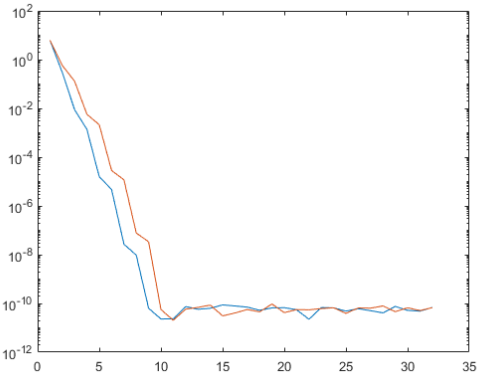

(D) Jellyfish

FIGURE 5: Other Area Tests

References

[1] Robert A. Adams and Christopher Essex. *Calculus A Complete Course: A Complete Course*. Pearson Education Canada, 2017.

[2] John P. Boyd. *Chebyshev & Fourier spectral methods*. Number 49 in Lecture notes in engineering. Springer, Berlin Heidelberg New York London Paris Tokyo Hong Kong, 1989.

[3] Philip J. Davis and Philip Rabinowitz. *Methods of numerical integration*. Computer science and applied mathematics. Academic Press, New York, 1975.

[4] Farikhin Farikhin and Ismail Mohd. Orthogonal Functions Based on Chebyshev Polynomials. *MATEMATIKA UTM*, 27:97–107, January 2011.

[5] Thomas C Hales. Jordan's Proof of the Jordan Curve Theorem.

[6] Alexander Keimer and Lukas Pflug. Modeling infectious diseases using integro-differential equations: Optimal control strategies for policy decisions and Applications in COVID-19. 2020. Publisher: Unpublished.

[7] Patrick Knupp and Stanly Steinberg. The Fundamentals of Grid Generation. 3, January 1993.

[8] David A. Kopriva. HOHQMesh, June 2023.

[9] J. C. Mason and D. C. Handscomb. *Chebyshev polynomials*. Chapman & Hall/CRC, Boca Raton, Fla, 2003.

[10] N. Papamichael and Nikos Stylianopoulos. *Numerical conformal mapping: domain decomposition and the mapping of quadrilaterals*. World Scientific, Hackensack, N.J, 2010. OCLC: ocn435420507.

[11] Lloyd N. Trefethen. Is Gauss Quadrature Better than Clenshaw–Curtis? *SIAM Review*, 50(1):67–87, January 2008.

[12] Lloyd N Trefethen. *Approximation Theory and Approximation Practice*. Siam, 2020.

[13] W. R. Wade. *Introduction to analysis*. Pearson Educational Limited, Harlow, fourth edition, pearson new international edition edition, 2014. OCLC: 955143383.

[14] Jörg Waldvogel. Fast Construction of the Fejér and Clenshaw–Curtis Quadrature Rules. *BIT Numerical Mathematics*, 46(1):195–202, March 2006.

[15] Shuhuang Xiang. On convergence rates of Fejér and Gauss–Chebyshev quadrature rules. *Journal of Mathematical Analysis and Applications*, 405(2):687–699, September 2013.

[16] Shuhuang Xiang, Xiaojun Chen, and Haiyong Wang. Error bounds for approximation in Chebyshev points. *Numerische Mathematik*, 116(3):463–491, September 2010.